Tunneling dynamics and phase transition of a Bose-Fermi mixture in a double well

Peng-Tang Qi and Wen-Shan Duan*

Department of Physics, Northwest Normal University, Lanzhou, 730070, People's Republic of China

(Received 10 March 2011; published 22 September 2011)

The coherent nonlinear tunneling dynamics of a boson-fermion mixture in a double-well potential is studied in this paper. Four types of phase are found for the mixture. The first one is two species localizing in different potential wells. The second one is two species coexisting in the same well. The third one is two species equally populated in two wells. The fourth one is one species equally populated in two wells while the other species is in one well. The phase transitions among these four states have been investigated. The interspecies and intraspecies interactions as well as bosonic and fermionic numbers can dramatically affect these phase transitions.

DOI: 10.1103/PhysRevA.84.033627 PACS number(s): 03.75.Mn

I. INTRODUCTION

Since the observation of molecules of Fermi atoms near Feshbach resonances, fascinating pairing correlations in cold Fermi gases have been successfully investigated both experimentally and theoretically [1–11]. An interesting issue is the inclusion of Bose atoms in the cold Fermi gases to form trapped boson-fermion mixtures such as ^{6}Li-^{23}Na, ^{40}K-^{87}Rb, and ^{6}Li-^{87}Rb, which have been experimentally observed [12–16] and theoretically studied [9–11]. The tunability of interspecies and intraspecies interactions via magnetic and optical Feshbach resonances makes the boson-fermion mixture a very attractive candidate for exploring new phenomena involving quantum coherence and nonlinearity.

During recent years, Bose-Einstein condensates (BECs) in double wells have offered a powerful tool to study the quantum tunneling phenomena [17–19] since almost every parameter, such as the interwell tunneling strength, onsite interaction strength, and the energy bias between the two wells, can be tuned experimentally [20]. There have been extensive studies on multispecies BEC in double wells [21]. Several interesting phenomena such as self-trapping (ST) and Josephson oscillation (JO) were studied both theoretically and experimentally [22–27]. The subject of this paper is an investigation of the tunneling dynamics of a boson-fermion mixture in a double-well potential. Our motivation is to explore whether new phenomena arise when there are interacting bosons and fermions trapped in symmetric double wells. The fermionic component is assumed to be in the superfluid state at unitarity or, alternatively, in the either BEC regime or Bardeen-Cooper-Schrieffer (BCS) regime. The system is made effectively one dimensional (1D), assuming that the gas is confined in transverse directions by a tight axisymmetric harmonic potential, with trapping frequencies $\omega_{\perp b}$ and $\omega_{\perp f}$ for the bosons and fermions respectively.

In the exploration of nonlinear tunneling dynamics of a boson-fermion mixture in a double well, JO, macroscopic quantum self-trapping (MQST), and phase separation (PS) are found. We sweep the parameter space and find the dependence of these phenomena on the system parameters. If the system is in the JO state, both population imbalances of bosons and fermions are in quasiperiodic oscillations with two competing frequencies. The two frequencies have been given analytically and numerically in the present study.

In Sec. II, the equations of the motion of the system are given. In Sec. III, the corresponding classical Hamiltonian and the fixed point are studied. In Sec. IV, small amplitude oscillations and their frequencies are given both analytically and numerically. In Sec. V, the tunneling dynamics is studied. The effects of interatomic interaction strength, bosonic number, and fermionic number to the tunneling dynamics are studied. The conclusions are given in Sec. VI.

II. EQUATION

We study a Bose-Fermi mixture composed of N_b condensed bosons of mass m_b and N_f fermions of mass m_f in two equally populated spinor components, at zero temperature. The set of coupled 1D equations for this system are as follows [11]:

$$i\frac{\partial\psi_b}{\partial t} = \left[-\frac{m_f}{m_b}\frac{\partial^2}{\partial x^2} + U_b(x) + g_b\,|\,\psi_b\,|^2 + g_{bf}N_f\,|\,\psi_f\,|^2\right]\psi_b, \tag{1}$$

$$\frac{i}{2}\frac{\partial\psi_f}{\partial t} = \left[-\frac{1}{8}\frac{\partial^2}{\partial x^2} + U_f(x) + g_f\,|\,\psi_f\,|^{4/3} + g_{bf}N_b\,|\,\psi_b\,|^2\right]\psi_f. \tag{2}$$

The $\psi_b(x,t)$ and $\psi_f(x,t)$ are order parameters of bosons and fermions respectively, $U_b(x)$ and $U_f(x)$ are the external potential acting on the bosons and fermions respectively, m_b and m_f are the masses of bosons and fermions respectively, $g_b = 2N_b(a_b/a_\perp)$ is the boson's self-interaction strength, $g_f = (3\pi^2)^{2/3}(3\xi/5)N_f^{2/3}$ is the fermions self-interaction strength, and $\xi = 1$ in the deep BCS regime and $\xi = 0.4$ at unitarity. $g_{bf} = 6a_{bf}/a_\perp$ is the interaction strength between boson and fermion, and a_b, a_f, and a_{bf} are the Bose-Bose scattering length, Fermi-Fermi scattering length, Bose-Fermi scattering length, respectively. We consider the special case of $a_\perp = a_{\perp b} = a_{\perp f}$, where $a_{\perp b} = \sqrt{\hbar/(m_b\omega_{\perp b})}$, $a_{\perp f} = \sqrt{\hbar/(m_f\omega_{\perp f})}$. Equations (1) and (2) are valid for the limited case of the weak coupling ($a_f \to 0, a_b \to 0$). In the 1D case of the BEC regime of the BEC-BCS crossover, both the transverse confinement

*duanws@nwnu.edu.cn

energies $\hbar\omega_{\perp f}$ and $\hbar\omega_{\perp b}$ must be much larger than the kinetic energy kT and the chemical potentials of μ_b and μ_f [9]. Our model is actually a special case of the US model reported in Ref. [9].

In the weakly linked limit, the dynamical oscillations of BEC and superfluid Fermi gas in double wells can be described by two wave functions representing the condensate in each trap. We then write the order parameters ψ_b and ψ_f as follows:

$$\psi_b = b_1(t)\varphi_1^b(x) + b_2(t)\varphi_2^b(x), \tag{3}$$

$$\psi_f = f_1(t)\varphi_1^f(x) + f_2(t)\varphi_2^f(x), \tag{4}$$

with $b_j(t) = \sqrt{N_j^b(t)}e^{i\theta_j^b(t)}$, $f_j(t) = \sqrt{N_j^f(t)}e^{i\theta_j^f(t)}$ $(j = 1,2)$, and constant total particle numbers (N), total bosonic numbers (N_b), total fermionic number (N_f), respectively, where $N_1^b + N_2^b = N_b$, $N_1^f + N_2^f = N_f$, and $N_b + N_f = N$. Defining the population imbalances and the relative phases as $s_b = \frac{N_2^b - N_1^b}{N_b}$, $s_f = \frac{N_2^f - N_1^f}{N_f}$, $\varphi_b = \theta_2^b - \theta_1^b$, and $\varphi_f = \theta_2^f - \theta_1^f$, we then obtain

$$\dot{s_b} = -2k_b\sqrt{1 - s_b^2}\sin\varphi_b, \tag{5}$$

$$\dot{s_f} = -2k_f\sqrt{1 - s_f^2}\sin\varphi_f, \tag{6}$$

$$\dot{\varphi_b} = \gamma_b + N_bU_bs_b + U_{bf}N_fs_f + 2k_b\frac{s_b}{\sqrt{1 - s_b^2}}\cos\varphi_b, \tag{7}$$

$$\dot{\varphi_f} = \gamma_f + \left(\frac{N_f}{2}\right)^{2/3}U_f[(1 + s_f)^{2/3} - (1 - s_f)^{2/3}] + U_{bf}N_bs_b + 2k_f\frac{s_f}{\sqrt{1 - s_f^2}}\cos\varphi_f, \tag{8}$$

where $\gamma_b = E_2^b - E_1^b$ and $\gamma_f = E_2^f - E_1^f$. The system parameters of k_b, k_f, γ_b, γ_f, U_b, U_f, and U_{bf} are all given in the appendix and can be adjusted in the experiments by using the external magnetic field (Feshbach resonance technique).

III. FIXED POINTS

The adiabatic evolution of quantum eigenstates correspond to the movement of fixed points determined by the classical Hamiltonian. The classical Hamiltonian, for the case of $N_b = N_f = N$ and $\gamma_b = \gamma_f = 0$, is

$$H = -2k_b\sqrt{1 - s_b^2}\cos\varphi_b - 2k_f\sqrt{1 - s_f^2}\cos\varphi_f + U_{bf}Ns_bs_f + \frac{NU_b}{2}s_b^2 + \frac{3}{5}\left(\frac{N}{2}\right)^{2/3}U_f[(1 + s_f)^{5/3} + (1 - s_f)^{5/3}]. \tag{9}$$

Equations (5), (6), (7) and (8) can then be written in the Hamiltonian form $\dot{s_b} = -\frac{\partial H}{\partial\varphi_b}$, $\dot{\varphi_b} = \frac{\partial H}{\partial s_b}$, $\dot{s_f} = -\frac{\partial H}{\partial\varphi_f}$, and $\dot{\varphi_f} = \frac{\partial H}{\partial s_f}$.

The fixed points can be given from the conditions of $\dot{s_b} = \dot{s_f} = \dot{\varphi_b} = \dot{\varphi_f} = 0$. The trivial solutions of the fixed points can be easily given as follows: $(s_b^f, \varphi_b^f, s_f^f, \varphi_f^f) = (0,0,0,0)$, $(0,\pi,0,\pi)$, $(0,0,0,\pi)$, and $(0,\pi,0,0)$, respectively. The nontrivial fixed points $s_b^f \neq 0$ and $s_f^f \neq 0$ result in a solution with population imbalance and lead to the tunneling dynamics with macroscopic self-trapping. The numerical solutions of the fixed points are shown in Fig. 1. In the region 1FP, there is only one fixed point of $s_b^f = 0, s_f^f = 0$; however, in the region 3FP there are three fixed points with nontrivial ones of $s_b^f \neq 0$ or $s_f^f \neq 0$. Actually there is also a five fixed points region (5FP), which is a very narrow region between 1FP and 3FP; see Fig. 1.

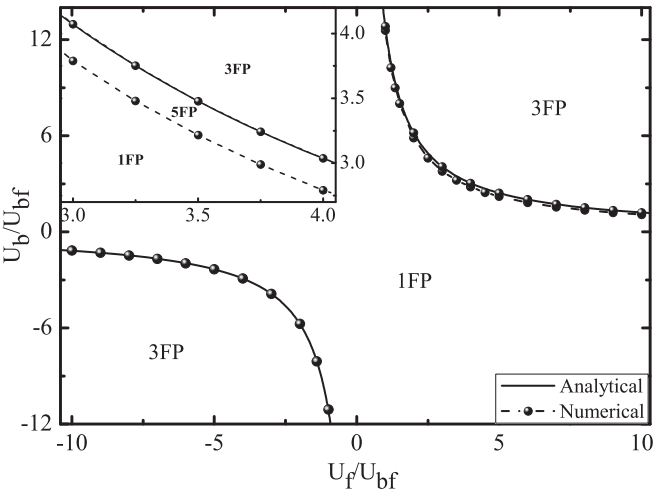

FIG. 1. Dependence of three different regions of one fixed point (1FP), three fixed points (3FP), and five fixed points (5FP) on the system parameters of U_b/U_{bf} and U_f/U_{bf}. The solid lines are the analytical results from Eq. (15).

IV. SMALL AMPLITUDE OSCILLATION AND THEIR OSCILLATION FREQUENCIES

We need to analyze the stability of fixed points in order to find out whether the requirement of adiabatic evolution of the system is fulfilled. To do this, we work with the differential equations (5), (6), (7), and (8). The infinitesimal variables of x_j and α_j $(j = b, f)$ are introduced by $s_j = s_j^f + x_j$ and $\varphi_j = \varphi_j^f + \alpha_j$, where s_j^f, φ_j^f are the fixed points. We only consider the simple case of $s_j^f = 0$. According to Eqs. (5), (6), (7), and (8), the linearized equations of motion are derived as follows:

$$\dot{x_j} = -2k_j\alpha_j, \tag{10}$$

$$\dot{\alpha_b} = N_bU_bx_b + N_fU_{bf}x_f + 2k_bx_b, \tag{11}$$

$$\dot{\alpha_f} = \frac{4}{3}\left(\frac{N_f}{2}\right)^{2/3}U_fx_f + N_bU_{bf}x_b + 2k_fx_f. \tag{12}$$

Based on these equations, we obtain

$$\frac{d^4x_b}{dt^4} + A\frac{d^2x_b}{dt^2} + Bx_b = 0, \tag{13}$$

where $A = 2k_b(N_bU_b + 2k_b) + 2k_f[\frac{4}{3}(\frac{N_f}{2})^{2/3}U_f + 2k_f]$ and $B = 4k_bk_f\{(N_bU_b+2k_b)[\frac{4}{3}(\frac{N_f}{2})^{2/3}U_f+2k_f]-N_bN_fU_{bf}^2\}$, we obtain the following equation from Eq. (13):

$$\lambda^2 = \tfrac{1}{2}[-A \pm \sqrt{A^2 - 4B}], \tag{14}$$

where the solutions of Eq. (13) are of the form $e^{\lambda t}$. In order to obtain the stable solutions the inequality $\lambda^2 \leqslant 0$ must be satisfied; otherwise, the solutions are unstable and the new fixed points of $s_b^f \neq 0$ or $s_f^f \neq 0$ appear. Therefore, we obtain the boundary line between one fixed point and five fixed points for the special case of $N_b = N_f = N$ as follows:

$$N^2 = \frac{4}{2^{2/3}3} N^{5/3} \frac{U_b}{U_{bf}} \frac{U_f}{U_{bf}} + 2N \frac{U_b}{U_{bf}} \frac{k_f}{U_{bf}} + \frac{8}{2^{2/3}3} N^{2/3} \frac{U_f}{U_{bf}} \frac{k_b}{U_{bf}} + 4 \frac{k_b}{U_{bf}} \frac{k_f}{U_{bf}}. \quad (15)$$

The analytical solutions of Eq. (15) are plotted in Fig. 1 in the solid line. Excellent agreement between the numerical results and the analytical ones is observed. If the condition of Eq. (14) is satisfied, two oscillation frequencies are given as follows:

$$\omega_1 = \frac{1}{\sqrt{2}} \sqrt{-A - \sqrt{A^2 - 4B}} \quad (16)$$

and

$$\omega_2 = \frac{1}{\sqrt{2}} \sqrt{-A + \sqrt{A^2 - 4B}}. \quad (17)$$

The Runge-Kutta method is used to obtain the numerical solutions of Eqs. (5), (6), (7), and (8).

Figure 2 shows the small amplitude oscillations of both fermionic and bosonic population imbalances between two wells with the initial conditions of $s_b(0) = s_f(0) = 0.01$, $\varphi_b(0) = \varphi_f(0) = 0$ and the interatomic interaction strength $U_b/U_{bf} = 3.5, U_f/U_{bf} = 5.0$. Such a mode exhibit quasiperiodic dynamics characterized by superposition of sinusoidal modes with two competing frequencies. The dependence of the two competing frequencies on the bosonic numbers (N_b) are given in Fig. 3. As clearly seen, ω_1 (the larger frequency) increases as the number of bosons increases. On the other hand, both frequencies of ω_1 and ω_2 increase as U_b increases [Fig. 3(a)]. Moreover, as the U_f increases ω_2 increase. However, ω_1 does not depend on U_f if N_b is not small enough; see Fig. 3(b). The excellent agreement between the analytical results of Eqs. (16) and (17) and the numerical ones are clearly shown in Fig. 3.

For the case shown in Fig. 2, both species of bosons and fermions execute small amplitude oscillations. The average values of population imbalances of both fermions and bosons with time are zero ($\overline{s_f} = \overline{s_b} = 0$), which indicates that there is no self-trapping; only Josephson oscillation exists. However, for other cases such as $U_b/U_{bf} = 8.0, U_f/U_{bf} = -1.5$ with the same initial condition (zero mode), the mean value of population imbalances of both fermions and bosons are nonzero. $\overline{s_b} < 0$, $\overline{s_f} > 0$ as shown in Fig. 4. It suggests that MQST phenomena happen with phase separation of two species. For the case of $U_b/U_{bf} = -3.5$, $U_f/U_{bf} = -3.1$ with the different initial conditions of $s_b(0) = s_f(0) = 0.01$, $\varphi_b(0) = \varphi_f(0) = \pi$ (π mode), which is shown in Fig. 5. The mean value of population imbalances of both fermions and bosons are nonzero. $\overline{s_b} > 0$, $\overline{s_f} > 0$ (both are positive), suggesting MQST happen but there is no phase separation.

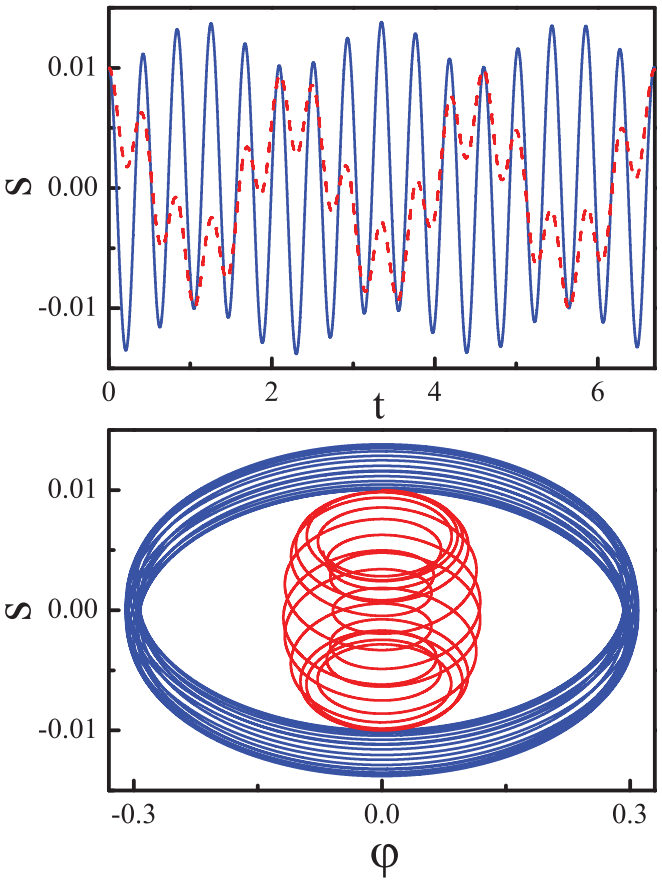

FIG. 2. (Color online) Time series of population imbalances (top) and phase portraits (bottom) for $U_b/U_{bf} = 3.5$, $U_f/U_{bf} = 5.0$ with initial condition $s_b(0) = s_f(0) = 0.01$ and $\varphi_b(0) = \varphi_f(0) = 0$. The red line (dashed, top, and inner, bottom) and blue line (solid, top, and outer, bottom) correspond to species of fermions and bosons respectively. The units of s and t are dimensionless, and the unit of φ is radian.

In the following section, we describe a detailed study about in what condition MQST and phase separation will happen and in what condition MQST and phase separation do not occur.

V. TUNNELING DYNAMICS OF FERMIONS

A. Effect of the interatomic interaction strength on the tunneling dynamics

1. Zero mode ($\overline{\varphi_b(t)} = \overline{\varphi_f(t)} = 0$)

We sweep the (U_b/U_{bf}, U_f/U_{bf}) parameter space in a large range with initial conditions of $s_b(0) = s_f(0) = 0.01$, $\varphi_b(0) = \varphi_f(0) = 0$, and $N_b = N_f$ and obtain the phase diagram shown in Fig. 6. We find that there are four regions denoted by self-trapping I (STI), self-trapping II (STII), chaos region (CR), and JO. In region STI, MQST appears accompanied by phase separation of two species since the mean population imbalances with time t of both fermions and bosons have opposite signs ($\overline{s_b} < 0$, $\overline{s_f} > 0$). Even with the initial conditions corresponding to an abundance of both species in the same well, the two components localize in two different wells. The typical time variations of both s_b and s_f

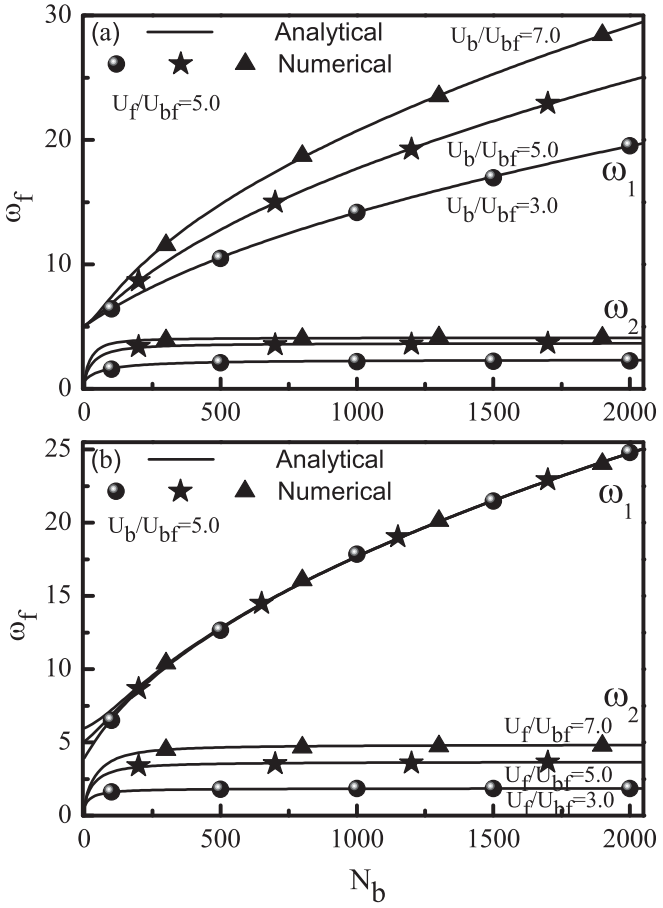

FIG. 3. Dependence of competing frequency ω_f on the total number of bosons in two wells. Frequencies are in units of $\omega_{\perp F}^{-1} = \omega_{\perp B}^{-1}$.

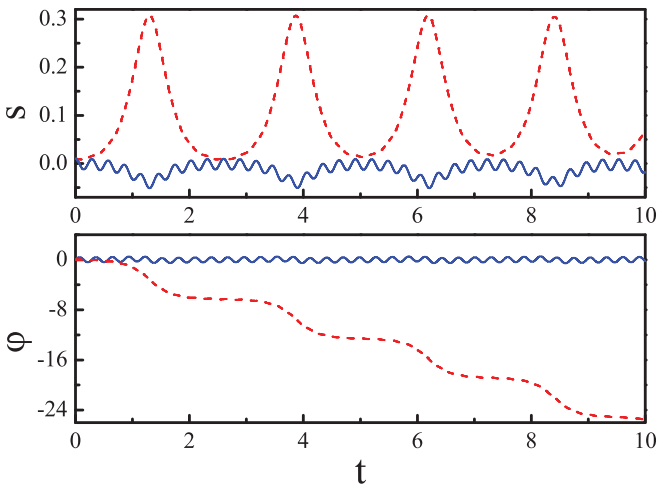

FIG. 4. (Color online) Time series of population imbalances (top) and phase differences (bottom) for $U_b/U_{bf} = 8.0$, $U_f/U_{bf} = -1.5$ with initial conditions $s_b(0) = s_f(0) = 0.01$ and $\varphi_b(0) = \varphi_f(0) = 0$. The dashed red line and solid blue line correspond to species of fermions and bosons respectively. The units of s and t are dimensionless, the unit of φ is radian.

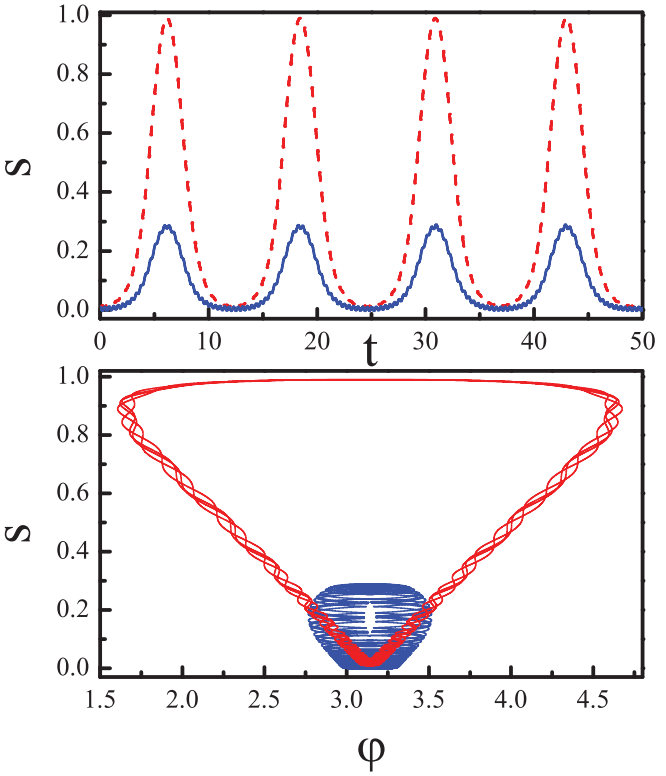

FIG. 5. (Color online) Time series of population imbalances (top) and phase portraits (bottom) for $U_b/U_{bf} = -3.5$, $U_f/U_{bf} = -3.1$ with initial conditions $s_b(0) = s_f(0) = 0.01$ and $\varphi_b(0) = \varphi_f(0) = \pi$. The red (dashed, top, and upper, bottom) line and blue line (solid, top, and lower, bottom) correspond to species of fermions and bosons respectively. The units of s and t are dimensionless, and the unit of φ is radian.

are shown in Fig. 4. In the region STII, MQST also takes place accompanied by phase separation, which is similar to that in region STI. The difference between the two regions is that the signs of $\overline{s_b}$ and $\overline{s_f}$ are different. $\overline{s_b} > 0$ and $\overline{s_f} < 0$. In region CR, MQST and phase separation may exist; however, the signs of either $\overline{s_b}$ or $\overline{s_f}$ have no regular pattern. In the region JO, $\overline{s_b} = \overline{s_f} = 0$, suggesting that there are no MQST and that only Josephson oscillations exist. The typical evolution of both s_f and s_b with time t are given in Fig. 2.

2. π mode ($\overline{\varphi_b(t)} = \overline{\varphi_f(t)} = \pi$)

We also sweep the parameter space (U_b/U_{bf}, U_f/U_{bf}) in a large range with initial conditions of $s_b(0) = s_f(0) = 0.01$, $\varphi_b(0) = \varphi_f(0) = \pi$, and $N_b = N_f$ and obtain the phase diagram shown in Fig. 7. We find that there are four regions denoted by same self-trapping (SST), one self-trapping (OST), CR, and JO. In region SST, MQST of both species takes place in the same well since the mean population imbalances with time t of both fermions and bosons have the same sign ($\overline{s_b} > 0$, $\overline{s_f} > 0$). The typical picture of this case is shown in Fig. 5. In the region OST, MQST takes place for only one species such as for fermions ($\overline{s_f} > 0$), but other species of bosons are in Josephson oscillation ($\overline{s_b} = 0$). In region CR, there is no regular pattern. In region JO, $\overline{s_b} = \overline{s_f} = 0$, suggesting that only Josephson oscillations exist.

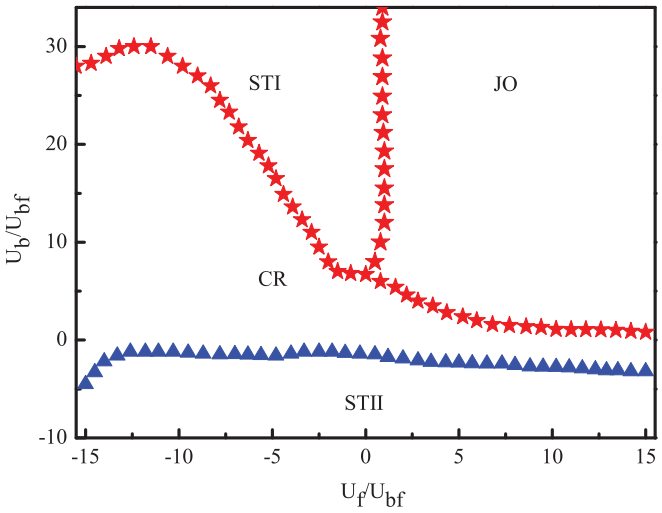

FIG. 6. (Color online) Dependence of four regions of STI, STII, CR, and JO on the system parameters of interatomic interactions of U_b/U_{bf} and U_f/U_{bf}. In region STI self-trapping appears; the bosons are in one well (for example, well 1) and the fermions are in the other well (well 2). Whether the bosons are in well 1 or well 2 depends on the initial conditions. In region STII self-trapping also appears; the bosons are in one well (well 2) while the fermions are in the other well (well 1). In region CR, there is no regular pattern. In region JO, the average population differences of both bosons and fermions are all zero; only Josephson oscillations exist, where the initial conditions are $s_b(0) = s_f(0) = 0.01$, $\varphi_b(0) = \varphi_f(0) = 0$, and $N_b = N_f$.

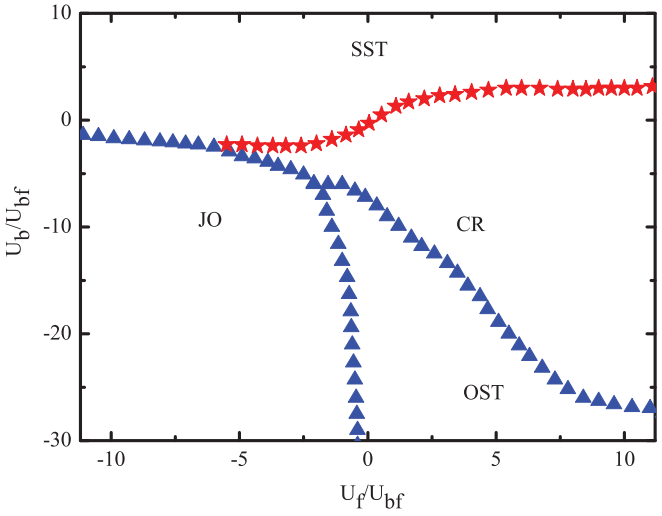

FIG. 7. (Color online) Dependence of four regions of SST, OST, CR, and JO on the system parameters of interatomic interactions of U_b/U_{bf} and U_f/U_{bf}. In region SST, self-trapping appears, and the bosons and fermions are in the same well. In region OST, self-trapping also appears, but only the fermions are in well 2 while the bosons are in Josephson oscillation. In region CR, an irregular oscillation pattern takes place. In region JO, the average population differences of both bosons and fermions are all zero, and only Josephson oscillations exist, where the initial conditions are $s_b(0) = s_f(0) = 0.01$, $\varphi_b(0) = \varphi_f(0) = \pi$, and $N_b = N_f$.

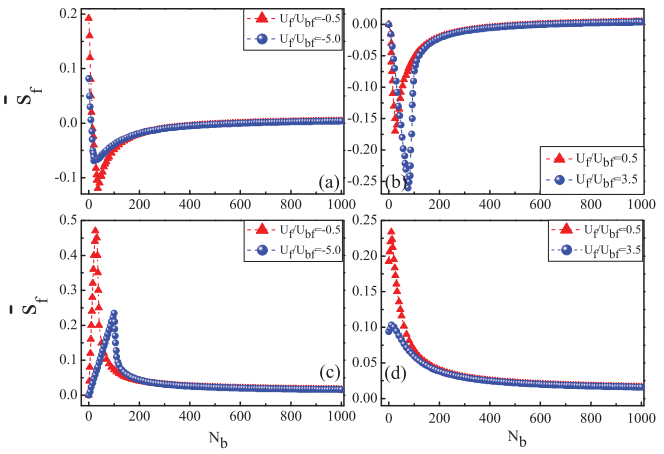

FIG. 8. (Color online) Dependence of the average population imbalance of fermions $\overline{s_f}$ between two wells on the bosonic numbers N_b for the different parameters of (a) $U_f/U_{bf} = -0.5, -5$, $\varphi_b(0) = \varphi_f(0) = 0$, (b) $U_f/U_{bf} = 0.5, 3.5$, $\varphi_b(0) = \varphi_f(0) = 0$, (c) $U_f/U_{bf} = -0.5, -5$, $\varphi_b(0) = \varphi_f(0) = \pi$, (d) $U_f/U_{bf} = 0.5, 3.5$, $\varphi_b(0) = \varphi_f(0) = \pi$. $N_f = 1000$, $s_b(0) = 0.99$, and $s_f(0) = 0.01$.

B. Effect of the bosonic numbers N_b on the tunneling dynamics of fermions

1. Zero mode

The initial conditions of the system in this case are $\varphi_b(0) = \varphi_f(0) = 0$, $s_f(0) = 0.01, s_b(0) = 0.99$. Figure 8 shows the dependence of $\overline{s_f}$ on the N_b. We note that $\overline{s_f} > 0$ if $N_b = 0$ and $U_f/U_{bf} < 0$, suggesting that the abundance of fermions is in one well [see Fig. 8(a)]. We can explain this phenomenon. For the case of zero mode, we note from Eq. (9) that the initial energy of the system is in its minimum value. For the attractive interaction, the system energy is small if the abundance of fermions is in one well. On the other hand, the system energy is in its minimum value if average population imbalance is zero for the repulsive interaction [see in Fig. 8(b)].

However, if bosons are injected in one well, the results are different. It seems that as the N_b increase the average population imbalance of fermions ($\overline{s_f}$) first decreases (self-trapping appears) until it reaches a minimum value $\overline{s_f}^{\min}$ and then increases gradually and approaches zero ($\overline{s_f} \to 0$) as N_b increases further [see Figs. 8(a) and 8(b)]. Figures 8(a) and 8(b) correspond to the attractive and repulsive interatomic interactions between fermions respectively. However, this minimum value of $\overline{s_f}^{\min}$ depends on the interatomic interaction strength of both U_b/U_{bf} and U_f/U_{bf}. The dependence of $\overline{s_f}^{\min}$ on the interaction parameters and the bosonic numbers N_b are given in Fig. 9(a).

2. π mode

The initial conditions of the system in this case are $\varphi_b(0) = \varphi_f(0) = \pi, s_f(0) = 0.01$, and $s_b(0) = 0.99$. We note that $\overline{s_f} = 0$ if $N_b = 0$ and $U_f/U_{bf} < 0$ [see Fig. 8(c)], which suggests that there is no self-trapping. The reason for this phenomenon is that for the π mode, the initial energy of the system is its maximum value. For the attractive interaction, the system energy is maximum if the fermions are equally populated

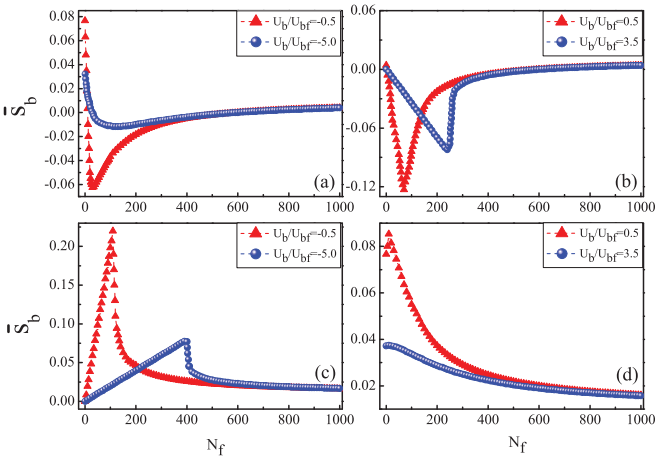

FIG. 9. (Color online) (a) The solid balls are the numerical results of the minimum points of the $\overline{s_f^{\min}}$, where $N_f = 1000, U_b/U_{bf} = 3.5, s_b(0) = 0.99, s_f(0) = 0.01$, and $\varphi_b(0) = \varphi_f(0) = 0$. (b) The solid balls are the numerical results of the maximum points of the $\overline{s_f^{\max}}$, $\varphi_b(0) = \varphi_f(0) = \pi$, and other system parameters are the same as in (a).

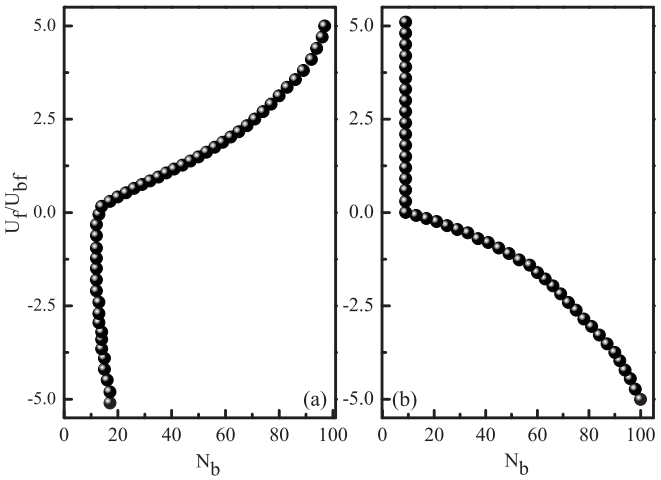

FIG. 10. Dependence of the average population imbalance of fermions $\overline{s_b}$ between two wells on the N_f for the different parameters of (a) $U_b/U_{bf} = -0.5, -5$, $\varphi_b(0) = \varphi_f(0) = 0$, (b) $U_b/U_{bf} = 0.5, 3.5$, $\varphi_b(0) = \varphi_f(0) = 0$, (c) $U_b/U_{bf} = -0.5, -5$, $\varphi_b(0) = \varphi_f(0) = \pi$, and (d) $U_b/U_{bf} = 0.5, 3.5$, $\varphi_b(0) = \varphi_f(0) = \pi$. $N_b = 1000$, $s_b(0) = 0.01, s_f(0) = 0.99$.

in two wells ($\overline{s_f} = 0$). However, the system energy is maximum if the abundance of fermions is in one well for the repulsive interaction [see in Fig. 8(d)].

If bosons are injected in one well, the situation is different. It is found from Figs. 8(c) and 8(d) that as the bosonic numbers N_b increase, $\overline{s_f}$ first increases (self-trapping appears) until a maximum value $\overline{s_f}^{\max}$, then decreases gradually and attends to zero ($\overline{s_f} \to 0$) as N_b increases further. Figures 8(c) and 8(d) are the results corresponding to the attractive and repulsive interactions between fermions respectively. The dependence of $\overline{s_f}^{\max}$ on the interaction parameters and the bosonic numbers N_b are given in Fig. 9(b).

C. Effect of the fermionic numbers N_f to the tunneling dynamics of bosons

1. Zero mode

The dependence of $\overline{s_b}$ on N_f is shown in Fig. 10. We note that $\overline{s_b} > 0$ if $N_f = 0$ [see Fig. 10(a)], indicating that the abundance of bosons is in one well. This phenomenon can be similarly explained. For the zero mode case, we note from Eq. (9) that the initial energy of the system is in its minimum value. The system energy is small if the abundance of fermions is in one well for the attractive interaction between bosons. On the other hand, if bosons are equally populated in two wells ($\overline{s_b} = 0$), the system energy is in its minimum values for the repulsive interaction between bosons [see in Fig. 10(b)].

However, if fermions are injected in one well, the results are completely different. If N_f are small enough [for example, $N_f < 300$ in Figs. 10(a) and 10(b)] $\overline{s_b}$ is nonzero, indicating that self-trapping appears. A minimum value of $\overline{s_b}$ will be reached for a certain value of N_f [see Figs. 10(a) and 10(b)]. As the N_f increases further, the average population imbalance of bosons ($\overline{s_b}$) increases gradually and finally approaches zero ($\overline{s_b} \to 0$) as N_f increases further [see Figs. 10(a) and 10(b)], which corresponds to the attractive and repulsive interatomic interaction between bosons respectively. The dependence of $\overline{s_b}^{\min}$ on the interaction parameters and the fermionic numbers N_f are given in Fig. 11(a).

2. π mode

Figure 10(c) show that $\overline{s_b} = 0$ if $N_f = 0$ and $U_f/U_{bf} < 0$, which indicates that there is no self-trapping in this case. The reason is that for the π mode the initial energy of the system is in its maximum value. For the attractive interaction between bosons, the system energy is in maximum value if the bosons are equally populated in two wells ($\overline{s_b} = 0$). However, the system energy is in its maximum value if the abundance of bosons is in one well for the repulsive interatomic interaction between bosons [see Fig. 10(d)].

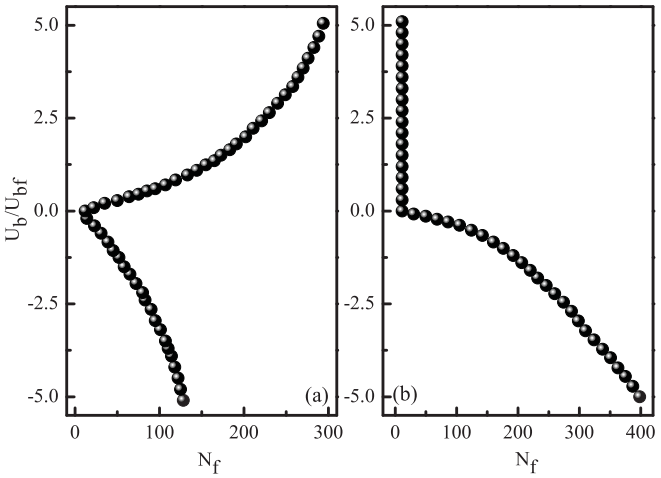

FIG. 11. (a) The solid balls are the numerical results of the minimum points of the $\overline{s_b^{\min}}$, where $N_b = 1000, U_f/U_{bf} = 3.5$, $s_f(0) = 0.99, s_b(0) = 0.01$, and $\varphi_b(0) = \varphi_f(0) = 0$. (b) The solid balls are the numerical results of the maximum points of the $\overline{s_b^{\max}}$, $\varphi_b(0) = \varphi_f(0) = \pi$, and other system parameters are the same as in (a).

If fermions are injected in one well, the results are completely different. It is found from Fig. 10(c) that as the fermionic number N_f increases, $\overline{s_b}$ first increases (self-trapping appears) until it reaches a maximum value $\overline{s_b}^{\max}$, then decreases gradually, and approaches zero ($\overline{s_b} \to 0$) as N_f increases further if the interaction between bosons is attractive. On the other hand, if the interaction between bosons is repulsive, shown in Fig. 10(d), we note that as N_f increases, $\overline{s_b}$ decreases gradually and then approaches zero. It seems that if the number of N_f is large enough, the bosons are in Josephson oscillation. The dependence of $\overline{s_b}^{\max}$ on the interaction parameters and the fermionic numbers N_f are given in Fig. 11(b).

VI. CONCLUSION

The tunneling dynamics of boson-fermion mixture in a double-well potential is investigated in the present paper. The fermionic component is assumed to be in the superfluid state at unitarity or in the BCS regime. We also assume that the mixture is confined in transverse directions by a tight axisymmetric harmonic potential. The Josephson oscillation, macroscopic quantum self-trapping, and PS are found for the mixture. By sweeping the parameter space, we find the dependence of these phenomena on the system parameters. If the system is in JO state, both population imbalances of bosons and fermions are in quasiperiodic oscillations with two competing frequencies. The two frequencies have been given analytically and numerically. The four types of phases of the mixture are found. The first one is that the two species localize in different potential wells. The second one is that the two species coexist in the same well. The third is that the two species are equally populated in two wells. The fourth one is that one species is equally populated in two wells, while the abundance of the other species is in one well. The phase transitions among these four states have been investigated. The interspecies and intraspecies interactions as well as bosonic and fermionic numbers can dramatically affect these phase transitions, which are numerically shown in the paper.

ACKNOWLEDGMENTS

The authors are grateful to the National Natural Science Foundation of China (Grant Nos. 91021021 and 10875098) and the Natural Science Foundation of Northwest Normal University (Grant No. NWNU-KJCXGC-03-48).

APPENDIX: DERIVATION OF EQS. (5)–(8)

By substituting Eqs. (3) and (4) into Eqs. (1) and (2) and using the conditions of $\int \varphi_j^b \varphi_k^b dx = \delta_{jk}$, $\int \varphi_j^f \varphi_k^f dx = \delta_{jk}$ and the definitions of $b_j(t) = \sqrt{N_j^b(t)} e^{i\theta_j^b(t)}$, $f_j(t) = \sqrt{N_j^f(t)} e^{i\theta_j^f(t)}$ ($j = 1,2$), we obtain

$$i\frac{\partial b_1}{\partial t} = [E_1^b + U_1^b N_1^b + U_{bf} N_1^f] b_1 + k_1^b b_2, \quad \text{(A1)}$$

$$i\frac{\partial b_2}{\partial t} = [E_2^b + U_2^b N_2^b + U_{bf} N_2^f] b_2 + k_2^b b_1, \quad \text{(A2)}$$

$$i\frac{\partial f_1}{\partial t} = [E_1^f + U_1^f (N_1^f)^{2/3} + U_{bf} N_1^b] f_1 + k_1^f f_2, \quad \text{(A3)}$$

$$i\frac{\partial f_2}{\partial t} = [E_2^f + U_2^f (N_2^f)^{2/3} + U_{bf} N_2^b] f_2 + k_2^f f_1, \quad \text{(A4)}$$

where

$$E_j^b = -\frac{mf}{m_b}\int \varphi_j^b \frac{\partial^2 \varphi_j^b}{\partial x^2} dx + \int \varphi_j^b U_b \varphi_j^b dx, \quad \text{(A5)}$$

$$E_j^f = -\frac{1}{4}\int \varphi_j^f \frac{\partial^2 \varphi_j^f}{\partial x^2} dx + \int \varphi_j^f U_f \varphi_j^f dx, \quad \text{(A6)}$$

$$k_j^b = -\frac{m_f}{m_b}\int \varphi_j^b \frac{\partial^2 \varphi_{3-j}^b}{\partial x^2} dx + \int \varphi_{3-j}^b U_b \varphi_j^b dx, \quad \text{(A7)}$$

$$k_j^f = -\frac{1}{4}\int \varphi_j^f \frac{\partial^2 \varphi_{3-j}^f}{\partial x^2} dx + 2\int \varphi_{3-j}^f U_f \varphi_j^f dx, \quad \text{(A8)}$$

$$U_j^b = g_b \int [\varphi_j^b]^3 dx, \quad \text{(A9)}$$

$$U_j^f = 2g_f \int [\varphi_j^f]^{8/3} dx, \quad \text{(A10)}$$

$$U_{bf} = 2N_f g_{bf} \int [\varphi_j^f]^2 [\varphi_j^b]^2 dx, \quad \text{(A11)}$$

where damping and finite temperature effects are ignored. E_j^b and E_j^f are the zero-point energies of bosons and fermions in each well, U_j^b, U_j^f are related to the atomic self-interaction energies, and k^b, k^f describe the amplitude of the tunneling superfluid fermions and bosons.

By using the definition of the population imbalances and the relative phases of $s_b = \frac{N_2^b - N_1^b}{N_b}$, $s_f = \frac{N_2^f - N_1^f}{N_f}$, $\varphi_b = \theta_2^b - \theta_1^b$, and $\varphi_f = \theta_2^f - \theta_1^f$, we finally obtain Eqs. (5)–(8).

[1] C. A. Regal *et al.*, Nature (London) **424**, 47 (2003); C. A. Regal, M. Greiner, and D. S. Jin, Phys. Rev. Lett. **92**, 040403 (2004).
[2] K. E. Strecker, G. B. Partridge, and R. G. Hulet, Phys. Rev. Lett. **91**, 080406 (2003).
[3] S. Jochim *et al.*, Phys. Rev. Lett. **91**, 240402 (2003).
[4] M. Zwierlein *et al.*, Phys. Rev. Lett. **91**, 250401 (2003).
[5] C. Chin *et al.*, Science **305**, 1128 (2004).
[6] M. Holland *et al.*, Phys. Rev. Lett. **87**, 120406 (2001); E. Timmermans *et al.*, Phys. Lett. A **285**, 228 (2001); Y. Ohashi and A. Griffin, Phys. Rev. Lett. **89**, 130402 (2002).
[7] T. L. Ho, Phys. Rev. Lett. **92**, 090402 (2004).
[8] A. V. Andreev, V. Gurarie, and L. Radzihovsky, Phys. Rev. Lett. **93**, 130402 (2004).
[9] S. K. Adhikari and L. Salasnich, Phys. Rev. A **78**, 043616 (2008).
[10] S. K. Adhikari, H. Lu, and H. Pu, Phys. Rev. A **80**, 063607 (2009).
[11] S. K. Adhikari, B. A. Malomed, L. Salasnich, and F. Toigo, Phys. Rev. A **81**, 053630 (2010).
[12] C. A. Stan *et al.*, Phys. Rev. Lett. **93**, 143001 (2004).

[13] S. Inouye *et al*., Phys. Rev. Lett. **93**, 183201 (2004).
[14] F. Ferlaino *et al*., Phys. Rev. A **73**, 040702 (2006).
[15] S. Ospelkaus *et al*., Phys. Rev. Lett. **97**, 120403 (2006).
[16] B. Deh *et al*., Phys. Rev. A **77**, 010701(R) (2008).
[17] M. Grifoni and P. Hänggi, Phys. Rep. **304**, 229 (1998).
[18] X. Q. Xu, L. H. Lu, and Y. Q. Li, Phys. Rev. A **78**, 043609 (2008).
[19] I. I. Satiji, R. Balakrishnan, P. Naudus, J. Heward, M. Edwards, and C. W. Clark, Phys. Rev. A **79**, 033616 (2009).
[20] G. F. Wang, D. F. Ye, L. B. Fu, X. Z. Chen, and J. Liu, Phys. Rev. A **74**, 033414 (2006).
[21] J. Liu *et al*., Phys. Rev. A **66**, 023404 (2002).
[22] A. Smerzi, S. Fantoni, S. Giovanazzi, and S. R. Shenoy, Phys. Rev. Lett. **79**, 4950 (1997).
[23] G. J. Milburn, J. Corney, E. M. Wright, and D. F. Walls, Phys. Rev. A **55**, 4318 (1997).
[24] S. Raghavan, A. Smerzi, S. Fantoni, and S. R. Shenoy, Phys. Rev. A **59**, 620 (1999).
[25] M. Albiez, R. Gati, J. Fölling, S. Hunsmann, M. Cristiani, and M. K. Oberthaler, Phys. Rev. Lett. **95**, 010402 (2005).
[26] R. Qi, X. L. Yu, Z. B. Li, and W. M. Liu, Phys. Rev. Lett. **102**, 185301 (2009).
[27] J. M. Zhang, W. M. Liu, and D. L. Zhou, Phys. Rev. A **77**, 033620 (2008).